Focal Nodular Hyperplasia: Morphologic and Functional Information from MR Imaging with Gadobenate Dimeglumine[1]

Luigi Grazioli, MD
Giovanni Morana, MD
Michael P. Federle, MD
Giuseppe Brancatelli, MD
Marco Testoni, MD
Miles A. Kirchin, PhD
Katiuscia Menni, MD
Lucio Olivetti, MD
Nicola Nicoli, MD
Carlo Procacci, MD

Index terms:
Gadobenate dimeglumine
Iron
Liver, focal nodular hyperplasia, 761.3198
Liver neoplasm, diagnosis, 761.3198
Liver neoplasm, MR, 761.121411, 761.121412
Magnetic resonance (MR), contrast media, 761.12143
Manganese

Published online before print
10.1148/radiol.2213010139
Radiology 2001; 221:731–739

Abbreviations:
FNH = focal nodular hyperplasia
Gd-BOPTA = gadobenate dimeglumine
GRE = gradient echo
SPIO = Superparamagnetic iron oxide

[1] From the Department of Radiology, University of Brescia, Spedali Civili di Brescia, Piazzale Spedali Civili 1, 25023 Brescia, Italy (L.G., K.M., L.O.); Departments of Radiology (G.M., M.T., C.P.) and Surgery (N.N.), University of Verona, Italy; Department of Radiology, University of Pittsburgh Medical Center, Pa (M.P.F., G.B.); and Bracco, Milan, Italy (M.A.K.). Received December 11, 2000; revision requested February 3, 2001; revision received April 23; accepted May 25. **Address correspondence to** L.G. (e-mail: *lgrazioli@yahoo.com*).

Author contributions:
Guarantors of integrity of entire study, L.G., G.M.; study concepts and design, L.G., G.M.; literature research, M.T., K.M.; clinical studies, L.O., C.P., L.G., G.M., M.T., K.M.; data acquisition and analysis/interpretation, L.G., G.M., M.T., K.M.; manuscript preparation, L.G., G.M., M.A.K.; manuscript definition of intellectual content, all authors; manuscript editing and revision/review, L.G., G.B., M.P.F.; manuscript final version approval, all authors.

PURPOSE: To determine whether gadobenate dimeglumine (Gd-BOPTA) is able to provide morphologic and functional information for characterization of focal nodular hyperplasia (FNH).

MATERIALS AND METHODS: Sixty-three consecutive patients with proved FNH were retrospectively examined. Magnetic resonance (MR) imaging with T2-weighted turbo spin-echo and T1-weighted gradient-echo sequences was performed. Images were acquired prior to and during the dynamic phase of contrast-material enhancement and 1-3 hours after administration of 0.1 mmol/kg Gd-BOPTA. Qualitative analysis of signal intensity and homogeneity on images in the various phases of the MR study and examination for the presence of central scar or atypical features were performed. On the basis of features observed in the precontrast and dynamic phases, lesions were defined as typical or atypical. Intensity and enhancement patterns of the lesions and scars were also evaluated in the delayed phase.

RESULTS: One hundred FNHs were depicted on MR images. Seventy-nine of 100 lesions demonstrated typical morphologic and enhancement characteristics. On delayed phase images, 72% of 100 FNHs appeared hyperintense; 21%, isointense; and 7%, slightly hypointense. The delayed pattern of enhancement was homogeneous, heterogeneous, and peripheral in 58%, 22%, and 20% of 100 FNHs, respectively. Atypical morphologic features and lesion and/or scar enhancement were observed in 21 of 100 FNHs. On delayed phase images, 76% of 100 atypical FNHs appeared hyperintense, 14% isointense, and 10% slightly hypointense. Hyperintensity and isointensity allowed the correct characterization in 90% of atypical FNHs.

CONCLUSION: Gd-BOPTA during both dynamic and delayed phases provides morphologic and functional information for the characterization of FNH.

Focal nodular hyperplasia (FNH) is a benign tumorlike hepatic lesion that is the result of a hyperplastic response to abnormal vasculature (1). Histologically, it is characterized by the presence of normal hepatocytes with a malformed biliary system that leads to a slowing of biliary excretion (2).

Sonographic features of FNH are nonspecific (3,4), whereas helical computed tomography (CT) is able to provide sufficient information for the diagnosis of FNH only when the lesion depicts typical features, such as a central scar and uniform hypervascularity (5).

Gadolinium contrast material–enhanced magnetic resonance (MR) imaging, in addition to precontrast T1- and T2-weighted imaging, offers slightly improved sensitivity and specificity for the diagnosis of FNH compared with CT (6–8). However, specific diagnosis of FNH may not be possible due to atypical CT and MR features, which have been reported in 12%–83% of cases (2,3,9,10). When the diagnosis of FNH is not certain, radionuclide

imaging or biopsy are often used, although even these techniques do not always give a definitive diagnosis (11).

Contrast agents with hepato-specific properties have been shown to increase the sensitivity of MR imaging for the detection of focal hepatic lesions (12–15), although the role of these agents in the characterization of focal lesions has yet to be fully elucidated. Gadobenate dimeglumine (Gd-BOPTA) (Multihance; Bracco Imaging, Milan, Italy) is a paramagnetic gadolinium-based contrast agent that, in common with other gadolinium agents, has a vascular-interstitial distribution in the first few minutes after injection. Thereafter, some 2%–4% of the administered dose is taken up by functioning hepatocytes and is excreted in the bile, while the remaining dose undergoes renal elimination in a manner similar to that of conventional gadolinium-based agents (16). The fraction taken up by the hepatocytes brings about a marked hyperintensity of the liver that persists for at least 120 minutes after the injection (17). The usefulness of Gd-BOPTA during the dynamic phase of contrast agent distribution has recently been reported (13,18,19). As yet however, little has been documented on the potential of delayed MR imaging with Gd-BOPTA for the characterization of focal lesions.

The purpose of this study was to describe the morphologic and functional characteristics of FNH after Gd-BOPTA administration.

MATERIALS AND METHODS

Study Population

Of 230 patients examined by using Gd-BOPTA–enhanced MR imaging for a known or suspected focal liver lesion, 63 patients were ultimately proved to have at least one FNH lesion. These 63 patients (51 women, 12 men; mean age, 36.8 years ± 10.8 [mean ± SD]; range, 7–60 years) were examined between February 1999 and October 2000 at two institutions. Of these patients, 29 presented with symptoms and clinical signs such as pain in the upper abdomen. The remaining 34 patients were asymptomatic; for these patients the presence of FNH was an incidental finding at abdominal imaging performed for other reasons. Twenty-five women had a history of oral contraceptive use for an average of 5.8 years ± 4.5; none of the men were using steroids. Two patients had a history of a kidney tumor, and one patient had clinical evidence of chronic hepatitis.

A total of 100 lesions were detected in the 63 patients included in the study. These lesions were characterized as FNHs at surgery (10 lesions in eight patients; two lobectomies, two bisegmentectomies, three segmentectomies, and one resection of pedunculated FNH), percutaneous biopsy (45 lesions in 37 patients), other diagnostic imaging procedure (technetium 99m diethyl-iminodiacetic acid nuclear medicine scan, helical CT, MR), and follow-up (45 lesions in 18 patients) for a minimum of 2 years.

MR Imaging Protocol

The same MR imaging protocol was used at both institutions. All patients underwent MR imaging with a superconducting imager (Symphony, Magnetom SP; Siemens, Erlangen, Germany) operating at 1.5 T. For 36 (57.1%) of 63 patients, a phased-array torso multicoil was used. For the remaining 27 (42.9%) patients a whole-body coil was used. MR imaging was performed by using T2-weighted turbo spin-echo sequences (4,000/108 [repetition time msec/echo time msec]) and T1-weighted gradient-echo (GRE) sequences (110–140/4; flip angle, 80°). Images were acquired prior to the administration of contrast agent in T2-weighted spin-echo and T1-weighted GRE imaging, during the dynamic phase of contrast enhancement following an intravenously administered bolus of 0.1 mmol Gd-BOPTA per kilogram of body weight. T1-weighted GRE images were acquired at 25–30 seconds (arterial phase), 70–90 seconds (portal venous phase), 3–5 minutes (equilibrium phase), and in a delayed phase following the administration of Gd-BOPTA (T1-weighted GRE images acquired at 1, 2, and 3 hours after the injection). In 15 patients (18 lesions), T1-weighted fat saturation GRE images in addition to conventional GRE images were acquired 3 hours after contrast agent injection. Acquisition of images at points as long as 3 hours after contrast agent injection was performed because the abnormal biliary excretion known to occur in FNH might theoretically result in a delayed elimination of Gd-BOPTA relative to that occurring from the adjacent parenchyma. The section thickness varied between 6 and 10 mm depending on the hepatic volume. The entire liver was imaged by using a single acquisition during a single breath hold. The study protocol was approved by the institutional review board, and written informed consent was obtained from every patient.

Image Analysis

All images from both institutions were evaluated independently by two radiologists (L.G., G.M.) with roughly equal experience (reader 1, 12 years; reader 2, 10 years). Qualitative analysis consisted of an assessment of the signal intensity and homogeneity on the image in the various phases of the MR study (before, during, and after Gd-BOPTA administration) and a determination of whether a central scar or atypical features were present. A consensus evaluation on the part of the two reviewers was performed for those images for which reader disagreements were present. Signal intensity was considered homogeneous when equal intensity was observed in all parts of the lesion with the exception of the central scar, when present.

On the basis of features observed in the precontrast and dynamic phases and of prior reports on the appearance and enhancement characteristics of FNH (5), the lesions were defined as either typical or atypical. They were also classified as small (≤3-cm diameter) or large (>3-cm diameter). Lesions were considered typical when they appeared as homogeneously isointense or slightly hyperintense on T2-weighted images and isointense or slightly hypointense on T1-weighted images before contrast material administration. Typical behavior during the dynamic phase of contrast enhancement was noted when the lesion demonstrated marked and homogeneous signal intensity enhancement during the arterial phase, rapid and homogeneous signal intensity washout during the portal venous phase, and signal isointensity (with the exception of the scar) during the equilibrium phase.

A typical scar was revealed as a hyperintense central stellate area on T2-weighted images and as a hypointense area on T1-weighted images. During the dynamic phase of contrast enhancement, a typical scar appeared as hypointense during the arterial and portal venous phases and slightly hyperintense during the equilibrium phase. The presence of a scar was considered necessary for the definition of a typical lesion only for lesions greater than 3 cm.

Finally, the enhancement of the lesions and scars was evaluated in the delayed phase at 1, 2, and 3 hours after contrast agent injection. Evaluation in this phase was performed on the basis of signal intensity and pattern of enhancement.

Atypical features of lesions consisted of the following: lesion heterogeneity, hy-

TABLE 1
Morphologic Characteristics and Enhancement Pattern of 100 FNHs on MR Images

	Precontrast Phase		Dynamic Phase T1-weighted			Delayed Phase T1-weighted		
Signal Intensity*	T2-weighted	T1-weighted	Arterial	Portal Venous	Equilibrium	1 Hour	2 Hour	3 Hour
Hyperintense	50	0	100	50	30	67	69	72
Isointense	33	20	0	49	69	25	23	21
Hypointense	0	62	0	1	1	8	8	7
Not visible	17	18	0	0	0	0	0	0
Total	100	100	100	100	100	100	100	100

Note.—Data are the number of lesions.
* Signal intensity of the FNH relative to that of the liver.

pointensity in the portal or equilibrium phases, the absence of a central scar in lesions greater than 3 cm, scar hypointensity on T2-weighted images, and scar hypointensity in the equilibrium phase following injection of contrast agent. Other atypical features included the presence of a pseudocapsule, which was observed as a complete hyperintense peri-lesional ring during the equilibrium phase, the presence of hemorrhage, and the presence of necrosis.

RESULTS

A total of 100 lesions between 0.6 and 10.0 cm (4.0 cm ± 2.2) in diameter were identified in 63 patients; 49 of 100 lesions were less than or equal to 3 cm in diameter; and 51 were larger than 3 cm in diameter. One lesion only was identified in 48 (76.2%) of 63 patients while multiple lesions (two to eight lesions) were identified in 15 (23.8%) of 63 patients.

Lesions and Enhancement

The MR imaging appearance and behavior of the lesions in the various phases are summarized in Table 1.

Precontrast phase.–A total of 17 (17%) of 100 FNHs on T2-weighted images and 18 (18%) of 100 FNHs on T1-weighted images were not identifiable either because of inherent isointensity with the surrounding normal parenchyma or because of the small size of the lesion (diameter, 2.3 cm ± 1.3; maximum, 5.5 cm; minimum, 0.6 cm). The signal intensity of the lesion was homogeneous in 82 (99%) of 83 lesions visible on T2-weighted images and in 81 (99%) of 82 lesions visible on precontrast T1-weighted images (Fig 1a, 1b). Heterogeneous signal intensity was noted for one lesion (9.0 cm in diameter) both on T2- and T1-weighted images. This was due to the presence of cystic areas with a fluid-fluid layer consistent with previous hemorrhage.

Postcontrast dynamic phase.—Hyperintensity was noted for all the lesions during the arterial phase, with the degree of enhancement varying from moderate to strong. A progressive reduction of signal intensity enhancement over time leading to isointensity in the portal venous and equilibrium phases (Fig 1c, 1d) (Table 2) was noted. In 99 of 100 lesions arterial phase enhancement was homogeneous (Fig 2a), while in one of 100 lesions it was heterogeneous. In the portal venous and equilibrium phases one lesion was hypointense and four lesions had a pseudocapsule (Fig 2b).

Postcontrast delayed phase.—Of 100 lesions, signal intensity was greater than that of the surrounding parenchyma for 67, 69, and 72 lesions at 1, 2, and 3 hours, respectively (Table 2). Generally, a greater signal intensity compared with that of the surrounding parenchyma was noted in the later (3 hours) images than in the images acquired at 1 and 2 hours after contrast agent injection. Signal intensity was isointense to the surrounding parenchyma in 25, 23, and 21 of 100 lesions at 1, 2, and 3 hours after contrast agent injection, respectively. Finally, slight hypointensity with respect to the surrounding parenchyma was noted for eight, eight, and seven of 100 lesions at 1, 2, and 3 hours after contrast agent injection, respectively. All lesions, including the hypointense ones, showed enhancement after Gd-BOPTA injection; for the hypointense lesions, the enhancement was slightly lower than that of the surrounding parenchyma. At 3 hours after contrast agent injection, the following three main patterns of enhancement were noted: homogeneous enhancement in 52 (56%) of 93 lesions (Figs 1e, 1f, 2c), heterogeneous enhancement in 24 (26%) of 93 lesions (Fig 3), and peripheral enhancement in 17 (18%) of 93 lesions (Fig 4b). For the seven hypointense lesions, homogeneous hypointensity was noted for three (43%) lesions, heterogeneous hypointensity was noted for two (28.5%) lesions, while in two (28.5%) lesions a central hypointensity with a peripheral isointensity was noted.

Scar

The behavior of the scar in the various phases of the examination is summarized in Table 2.

Precontrast.—On T2-weighted images a scar was visible in 25 (25%) of 100 lesions; in 24 FNHs the scar was hyperintense, and in the other, it was hypointense. On T1-weighted images, a scar was visible in 36 of 100 FNHs in each instance as a hypointense area.

Postcontrast dynamic phase.—In the arterial phase, a scar was recognizable in 43 of 100 FNHs as a hypointense area. In the portal venous phase 28 scars remained hypointense, while 10 became isointense, and four became hyperintense. Finally, in the equilibrium phase, six scars appeared slightly hypointense, five isointense, and 35 hyperintense (Fig 1d).

Postcontrast delayed phase.—In the delayed phase, the visualization of the scars was improved; a central scar was noted in 53 of 100 FNHs overall. At 1 hour after contrast agent administration 50 of these 53 scars appeared hypointense while, at 2 and 3 hours after contrast agent administration all 53 scars appeared hypointense (Fig 1e). In 11 (22%) of 51 lesions, with a diameter greater than 3 cm, a scar was not recognizable in any phase of the examination. In the 49 lesions equal to or smaller than 3 cm in diameter; no scar was depicted on precontrast images in 44 (90%) lesions. On precontrast and postcontrast dynamic phase images combined, a scar was observed in seven of 49 (14%) lesions, while on postcontrast delayed phase images (1–3 hours after contrast agent injection) a scar was noted in 15 (31%) of 49 lesions (Fig 4).

Typical FNH

Precontrast and postcontrast dynamic phases.—A total of 79 (79%) of 100 lesions demonstrated typical morphologic and enhancement characteristics. Among 49 lesions (≤3 cm in diameter), 42 (80%) did not depict a central scar. Because small FNHs often lack a visible central scar, we did not classify these as atypical.

Delayed phase.—Of 79 FNHs on 3-hour

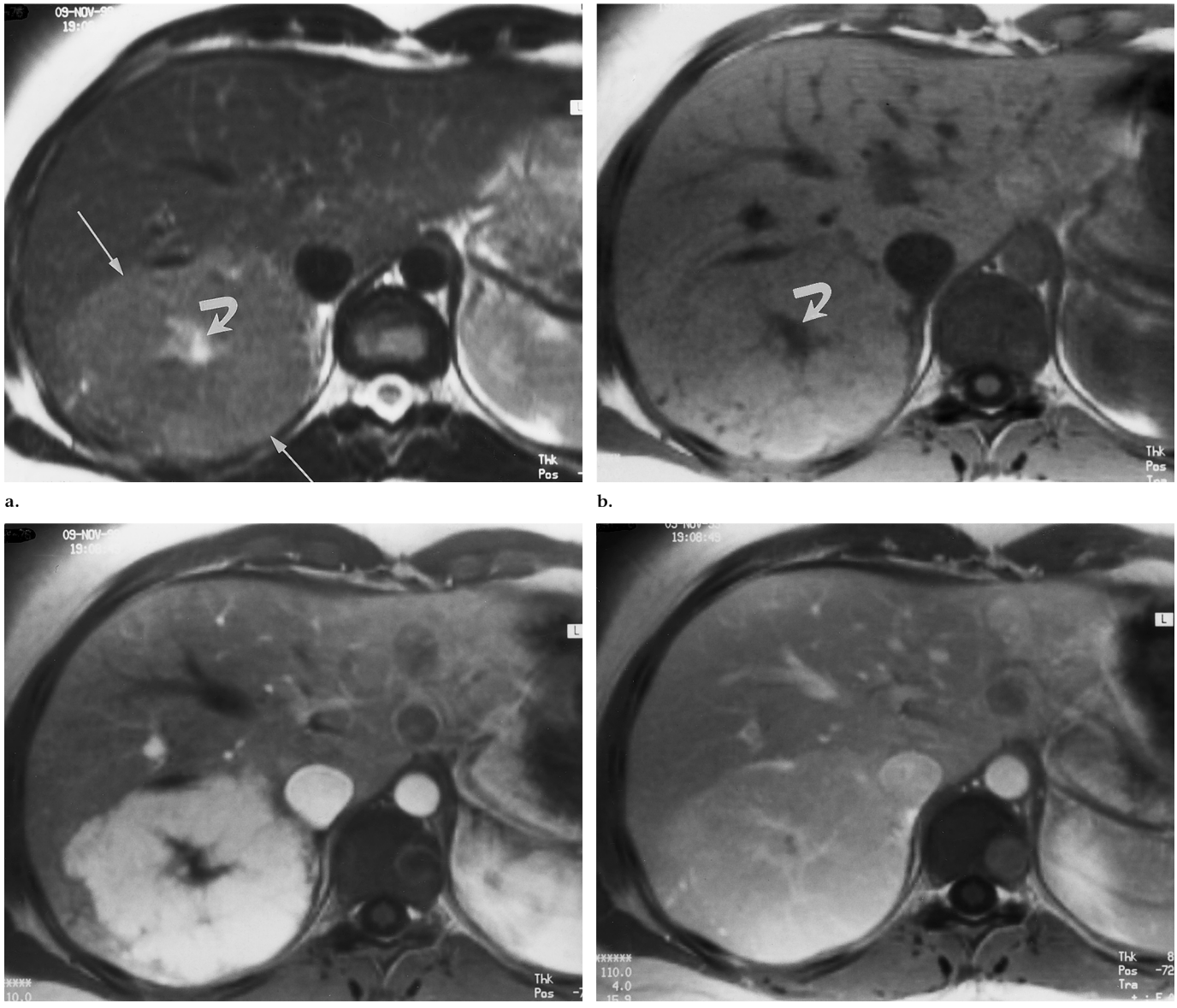

Figure 1. Chronic right upper abdominal pain in a 31-year-old woman. **(a)** Transverse turbo spin-echo T2-weighted (4,000/102) MR image shows a large and homogeneous slightly hyperintense lesion (arrows) in the right lobe of the liver. Central stellate scar (curved arrow) is hyperintense. **(b–e)** Transverse GRE T1-weighted (110/4; flip angle, 80°) MR images. **(b)** Precontrast image of the lesion is homogeneously isointense to the surrounding liver parenchyma; central scar (curved arrow) is hypointense. **(c)** Arterial phase image obtained 25 seconds after administration of Gd-BOPTA. Lesion is hyperintense and homogeneous; central scar is hypointense. **(d)** Equilibrium phase image obtained 5 minutes after administration of Gd-BOPTA. Lesion is slightly hyperintense to adjacent liver parenchyma; central scar is hyperintense. *(Fig 1 continues.)*

postcontrast images, 56 (71%) appeared hyperintense, 18 (23%) appeared isointense and five (6%) appeared slightly hypointense. The delayed enhancement pattern of 74 FNHs was homogeneous in 46 (62%), heterogeneous in 12 (16%), and peripheral in 16 (22%).

Atypical FNH

Precontrast and postcontrast dynamic phases.—In 21 (21%) of 100 FNHs atypical features associated with morphologic characteristics, lesion enhancement, or central scar enhancement were observed. These features made characterization of the lesions more difficult (Table 3). In one lesion the signal intensity was lower than that of the surrounding parenchyma in the equilibrium phase. In 11 (22%) of 51 FNHs greater than 3 cm in diameter, a central scar was not observed. In one lesion, a central scar appeared hypointense on precontrast T2-weighted images. Similarly, a hypointense scar was noted in the postcontrast equilibrium phase in six lesions. In four lesions, a pseudocapsule was observed; in three of these lesions, no central scar was present. Finally, one lesion was heterogeneous due to a previous hemorrhage.

Delayed phase.—Of 21 atypical FNHs on 3-hour postcontrast images, 16 (76%) appeared hyperintense, three (14%) became isointense, and two (10%) appeared slightly hypointense. The enhancement pattern was homogeneous in nine (47%)

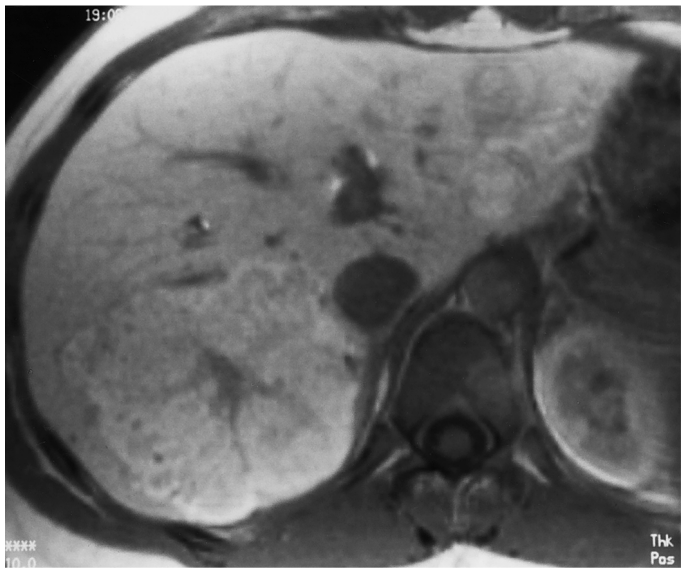

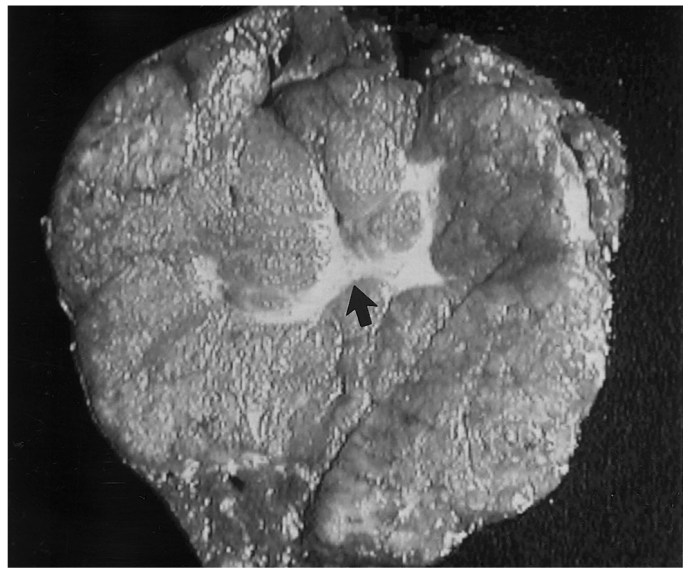

e. **f.**

Figure 1. (*continued*). **(e)** Image obtained 3 hours after administration of Gd-BOPTA. Nodule appears homogeneously hyperintense; scar is hypointense. **(f)** Cut surface of pathologic specimen demonstrates homogeneous tissue component of the lesion and large stellate fibrous central scar (arrow).

TABLE 2
Morphologic Characteristics and Enhancement Pattern of the Central Scar on MR Images

	Precontrast Phase		Dynamic Phase T1-weighted			Delayed Phase T1-weighted		
Signal Intensity*	T2-weighted	T1-weighted	Arterial	Portal Venous	Equilibrium	1 Hour	2 Hour	3 Hour
Hyperintense	24	0	0	4	35	0	0	0
Isointense	0	0	0	10	5	3	0	0
Hypointense	1	36	43	28	6	50	53	53
Not visible	75	64	57	58	54	47	47	47
Total	100	100	100	100	100	100	100	100

Note.—Data are the number of central scars out of 100 FNHs.
* Signal intensity of the scar relative to that of the lesion.

of the 19 isointense and hyperintense nodules, heterogeneous in seven (37%), and peripheral in three (16%).

Reader Disagreements

Reader disagreement with regard to signal intensity in the delayed phase (isointensity vs slight hyperintensity) occurred in three instances. After a consensus evaluation, two lesions were considered to be slightly hyperintense and one lesion to be isointense to the surrounding parenchyma. Disagreement also occurred in two instances with regards to atypical findings. In one instance, there was disagreement as to whether lesion hypointensity in the equilibrium phase should be considered typical or atypical; consensus judged it to be atypical (patient 1, Table 3). In the other instance, a small scar that was hypointense on T2-weighted images was recognized as atypical by consensus (patient 18, Table 3).

DISCUSSION

FNH is the second most common lesion of the liver after hemangioma. It is present in 3%–5% of the population and is more common in women of childbearing age (20).

Sonography is often used for the depiction of FNH, despite the fact that this technique does not provide specific and confident characterization of lesions in most patients. Helical CT with arterial and portal venous phase imaging offers confident depiction of FNH in many cases, but atypical features may make specific diagnosis difficult (2,3,9,10). Radionuclide imaging with sulfur colloid is generally considered useful in the characterization of FNH due to the uptake of tracer by the Kupffer cells. However, uptake is seen in only approximately two-thirds of lesions (2) and is limited to the detection only of large lesions.

The use of contrast-enhanced dynamic phase MR imaging, with traditional extracellularly distributed gadolinium-based contrast agents, provides the greatest diagnostic sensitivity among the techniques in current use, particularly when combined with the information available on precontrast T1- and T2-weighted images (6). Nevertheless, the presence of atypical features does not permit accurate characterization of FNH in every case, and current diagnosis at MR imaging relies on the same morphologic and hemodynamic features as helical CT.

The availability of novel liver-specific MR contrast agents increases the potential for accurate lesion characterization (21,22). Gd-BOPTA is a paramagnetic gadolinium-based contrast agent that behaves in a manner analogous to that of other gadolinium-based agents during the vascular-interstitial phase, in the first minutes after injection, and as an agent with liver-specific properties in a later delayed phase (16,17). Gd-BOPTA possesses increased in vivo relaxivity compared

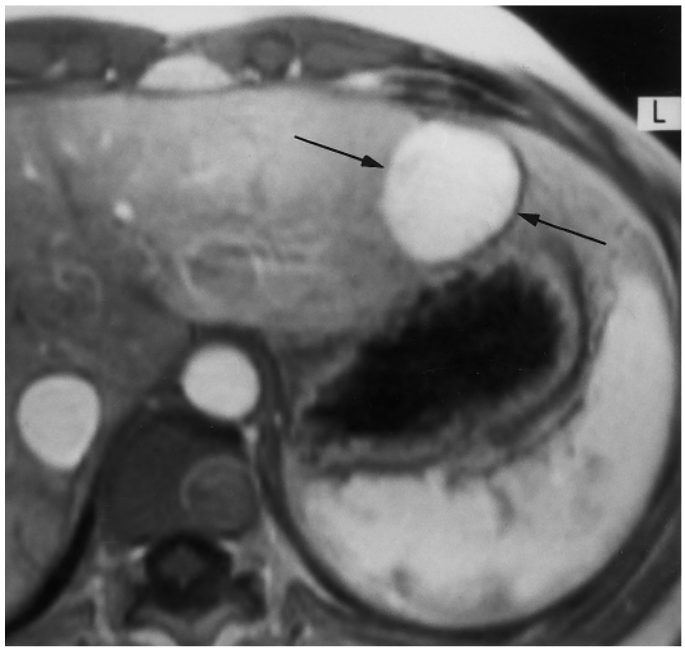

a.

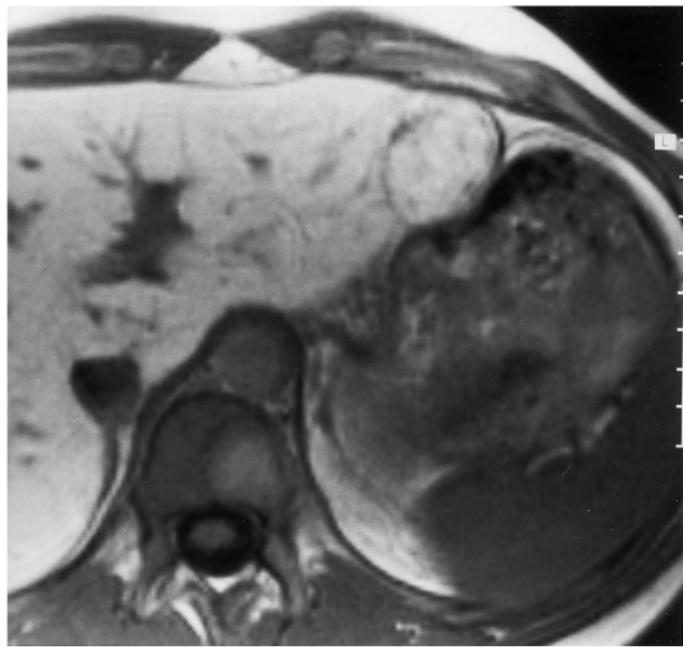

c.

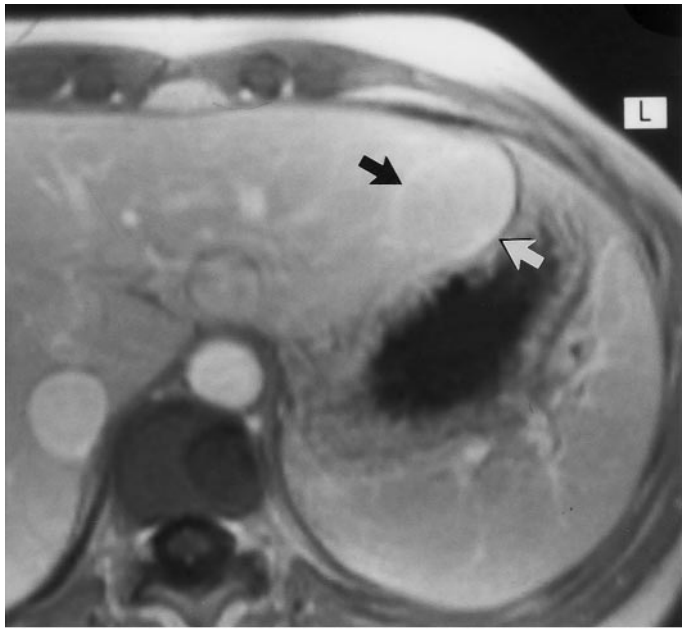

b.

Figure 2. MR images in a 27-year-old asymptomatic woman. Transverse GRE T1-weighted (120/4; flip angle, 80°) MR images. **(a)** Arterial phase image obtained 25 seconds after administration of Gd-BOPTA. The nodule (arrows) located in lateral segment of the liver shows homogeneous and intense enhancement. No central scar is evident. **(b)** Equilibrium phase image obtained 5 minutes after administration of Gd-BOPTA. Nodule appears slightly hyperintense and delimited by a thin hyperintense rim (arrows). **(c)** Image obtained 3 hours after administration of Gd-BOPTA. Nodule is slightly and homogeneously hyperintense.

with other gadolinium-based agents, and, unlike purely liver-specific agents, this agent can be administered as a rapid intravenous bolus to study the early distribution in the liver (17,23,24). The amount of Gd-BOPTA uptake into the hepatocytes (2%–4%) and the increased relaxivity of the molecule leads to a marked increase in liver parenchymal signal intensity (17), which has previously been shown to facilitate the improved detection of hepatic metastases (12,13,16, 19,25). Recently, delayed phase imaging with Gd-BOPTA has been shown to be of benefit for the characterization of hepatocellular carcinoma (26).

FNH is a benign lesion of hepatocellular origin which can provide an important test for such a contrast agent; the cellular structure of FNH is similar to that of normal hepatic parenchyma apart from the presence of an abnormal biliary system. The use of radionuclide imaging with tracers that simulate the behavior of bilirubin, such as ^{99m}Tc diethyl-iminodiacetic acid, may reveal the uptake and delayed excretion in FNH as a "hot spot" (2). However, the use of Gd-BOPTA permits both morphologic and functional information to be obtained, with the advantage of greater spatial resolution than that achievable with nuclear scintigraphy.

In the present study, 72 of 100 lesions were hyperintense in the delayed phase after injection of Gd-BOPTA. This can be considered analogous to the "hot spots" observed at scintigraphy. A further 21 lesions were isointense, while only seven of 100 lesions were slightly hypointense. The hyperintensity of the lesions permitted the correct characterization of 19 of 21 FNHs that, on precontrast and postcontrast dynamic phase images, presented sufficiently atypical morphologic features as to prevent a definitive diagnosis.

For FNHs that have atypical features at MR imaging or other imaging tests and for small lesions (≤3 cm), Gd-BOPTA–enhanced MR with delayed imaging provides valuable information. In our series, 21 of 100 FNHs were considered to have

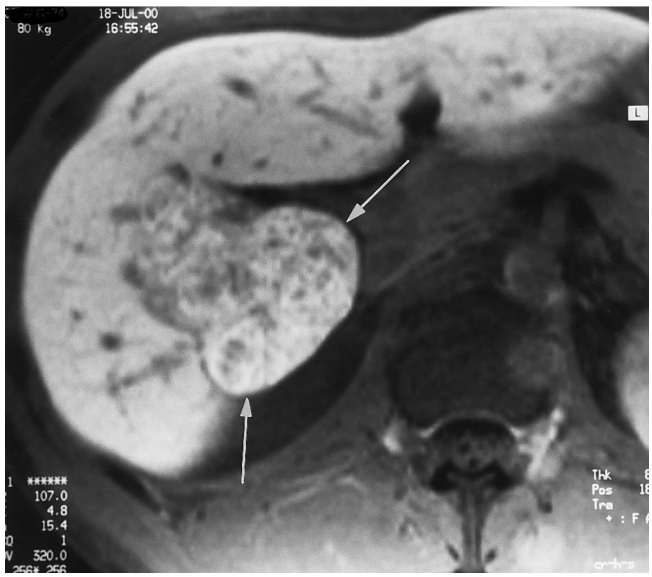

Figure 3. Transverse GRE T1-weighted (107/4.8; flip angle, 80°) fat-suppression MR image obtained in a 36-year-old man with intermittent right flank pain 3 hours after administration of Gd-BOPTA. Large partially exophytic mass (arrows) located in the right lobe of the liver shows heterogeneous hyperintensity.

TABLE 3
Atypical Findings in FNHs on MR Images

Patient No.	Atypical Findings	Enhancement Pattern of Lesions on Delayed Phase Images		
		1 Hour	2 Hour	3 Hour
1	Hypo in equilibrium phase	Iso	Iso	Iso
2	Hemorrhage and calcifications	Iso	Iso	Hyper
3	Pseudocapsule	Hyper	Hyper	Hyper
4	No scar	Hyper	Hyper	Hyper
5	No scar	Hyper	Hyper	Hyper
6	No scar	Iso	Iso	Iso
7	No scar	Hyper	Hyper	Hyper
8	No scar	Hyper	Hyper	Hyper
9	No scar	Hyper	Hyper	Hyper
10	No scar	Hyper	Hyper	Hyper
11	No scar; pseudocapsule	Iso	Iso	Iso
12	No scar; pseudocapsule	Hyper	Hyper	Hyper
13	Scar hypo in equilibrium phase	Hyper	Hyper	Hyper
14	Scar hypo in equilibrium phase	Hyper	Hyper	Hyper
15	Scar hypo in equilibrium phase	Hyper	Hyper	Hyper
16	Scar hypo in equilibrium phase	Hyper	Hyper	Hyper
17	Scar hypo in equilibrium phase	Hyper	Hyper	Hyper
18	Scar hypo in T2-weighted phase	Hypo	Iso	Hyper
19	Scar hypo in equilibrium phase	Hyper	Hyper	Hyper
20	No scar; pseudocapsule	Hypo	Hypo	Hypo
21	No scar	Hypo	Hypo	Hypo

Note.—Hyper = hyperintense, Iso = isointense, Hypo = hypointense.

atypical morphologic or lesion enhancement, making the diagnosis of FNH more difficult. Among these 21 instances, delayed enhanced images (3 hours) showed hyperintense (76%) or isointense (14%) enhancement of the FNH, which permitted a confident diagnosis.

The majority of small (≤3-cm) FNHs (42 [86%] of 49), did not have a visible scar on precontrast or dynamic enhanced images. Other investigators (2,3,5,9,10) have reported similar findings on MR and CT images. While the absence of a scar in small FNHs cannot be considered atypical, it does make it more difficult to distinguish FNH from other hypervascular neoplasms. Again, delayed phase imaging proved useful; all 49 small FNHs showed either hyperintense (33 [67%] lesions) or isointense (16 [33%] lesions) enhancement. In addition, a central scar was detected on delayed images in 15 (31%) of the 49 lesions compared with only seven (14%) of 49 on dynamic phase images.

Considering all 100 FNHs, delayed phase MR imaging permitted confident diagnosis of 93 FNHs. On T1-weighted images, the central scar appeared hypointense with precontrast and dynamic and delayed enhanced MR imaging. This reflects the biologic distribution of the Gd-BOPTA molecule, which accumulates selectively in hepatocytes. In FNH, there is prolonged and excessive hepatocellular accumulation of the contrast agent because FNH lacks a well-formed bile canalicular system to permit normal excretion (2,5).

Whether Gd-BOPTA–enhanced MR imaging will facilitate distinction of FNH from other neoplasms of hepatocellular origin is an important but unresolved question. A principal limitation of the present study is the absence of a blinded comparison with other hypervascular lesions. Work is ongoing to determine the sensitivity and specificity of delayed enhancement for the differential diagnosis of benign and malignant hypervascular liver lesions. The accumulation of the agent in hepatocellular carcinoma has been shown to correlate with the residual hepatocytic function in the neoplastic cells, as judged by the presence of bile in the neoplasm. In a prior report (26), only one of 34 hepatocellular carcinoma lesions demonstrated hyperintensity on delayed images following Gd-BOPTA. We are unaware of any specific study of the appearance of hepatocellular adenoma with Gd-BOPTA–enhanced MR. Our anecdotal experience with four cases of adenoma and one of adenomatosis (unpublished data) demonstrated much less intense enhancement of the adenoma on dynamic phase MR images and a markedly hypointense appearance on delayed images relative to FNH or normal liver. Although adenomas have functioning hepatocytes, they lack bile ducts. It is therefore likely that bilirubin metabolism is blocked in the adenoma, as confirmed by absence of bile in resected adenomas (27). Altered hepatocellular metabolism may inhibit the uptake of Gd-BOPTA in the adenoma thereby accounting for its hypointense appearance on delayed MR images. We also have anecdotal experience with three cases of fibrolamellar hepatocellular carcinoma; none of these tumors showed delayed en-

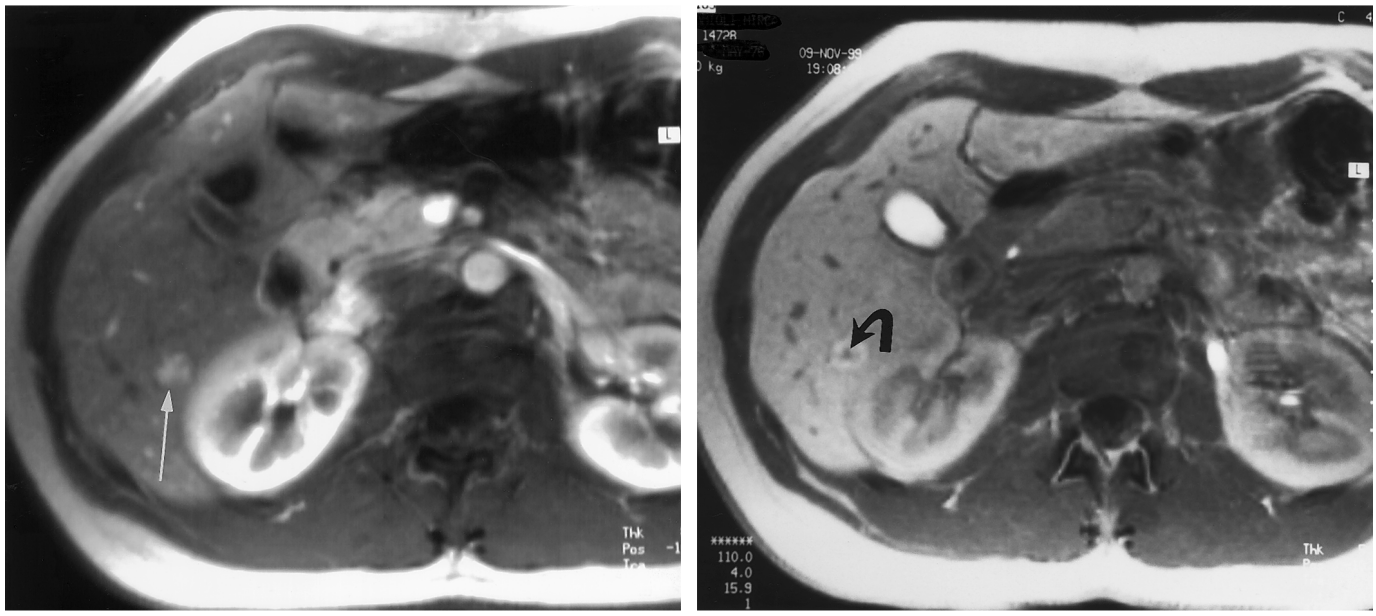

a. **b.**

Figure 4. Transverse GRE T1-weighted (120/4; flip angle, 80°) MR images in same patient as in Figure 1. **(a)** Arterial phase image obtained 25 seconds after bolus administration of Gd-BOPTA. A 1-cm homogeneous hyperintense nodule (arrow) is shown, with no central scar visualized. **(b)** Image obtained 3 hours after administration of Gd-BOPTA shows peripheral enhancement due to the presence of a large round central scar (curved arrow).

hancement on Gd-BOPTA-enhanced MR images.

Other liver-specific MR contrast agents are available. Manganese diproxyl diphosphate (mangafodipir trisodium Teslascan; Nycomed-Amersham, Princeton, NJ) is a recently developed hepatobiliary MR contrast agent that improves the detection of liver metastases due to selective enhancement of functioning hepatocytes. Potential disadvantages of mangafodipir include its uptake and enhancement by some benign and malignant (hepatocellular carcinoma) hepatic neoplasms, limiting its ability to characterize some hepatic lesions (21,28).

Superparamagnetic iron oxides (SPIO) (Feridex; Advanced Magnetics, Princeton, NJ and Endorem; Laboratoire Guerbet, Roissy, France) are superparamagnetic liver-specific contrast agents. When intravenously administered, they are extracted from the intravascular space by the reticulo-endothelial system and deposited mainly in the Kupffer cells. Enhancement by using SPIO alters the signal intensity of normal liver, but not the signal intensity of neoplasms, which lack Kupffer cells, and should increase depiction of liver metastases (14).

Kupffer cells are usually observed in FNH, and, along with malformed biliary ducts, are a major histologic feature of this lesion. Uptake of SPIO by FNH is therefore common (22). However, some lesions that lack Kupffer cells, including hemangioma and adenoma, have been reported (29) to demonstrate uptake of SPIO also. This appears to be due to pooling of the contrast agent in the vascular pools and peliosis-like dilatated vessels that characterize hemangiomas and adenomas, respectively (29).

It is important to note that neither mangafodipir nor SPIO have been documented to be safe and effective as a bolus contrast agent injection, making them ineffective for demonstration of the vascular and interstitial phases of liver lesion enhancement.

Further work might be usefully directed toward comparing the imaging features of FNH after Gd-BOPTA administration with those observed after administration of SPIO or mangafodipir. Similarly, a direct comparison of Gd-BOPTA–enhanced MR imaging of FNH with other imaging techniques, such as nuclear scintigraphy, is warranted.

In summary, Gd-BOPTA is a useful contrast agent for the study of FNH, offering opportunities during both the dynamic and delayed phases of contrast enhancement to acquire morphologic and functional information for the characterization of these lesions. Our experience suggests that the MR protocol should include T2-weighted turbo spin-echo sequences and T1-weighted GRE images acquired prior to and during the dynamic phase of an intravenously administered bolus of this agent. Delayed imaging (3 hours) provides important information when the other MR sequences do not reveal a specific diagnosis. MR imaging with Gd-BOPTA should be considered whenever FNH is suspected in a patient.

References

1. Wanless IR, Mawdsley C, Adams R. On the pathogenesis of focal nodular hyperplasia of the liver. Hepatology 1985; 5:1194–1200.
2. Boulahdour H, Cherqui D, Charlotte F, et al. The hot spot hepatobiliary scan in focal nodular hyperplasia. J Nucl Med 1993; 34:2105–2110.
3. Cherqui D, Rahmouni A, Charlotte F, et al. Management of focal nodular hyperplasia and hepatocellular adenoma in young women: a series of 41 patients with clinical, radiological, and pathological correlations. Hepatology 1995; 22:1674–1681.
4. Welch TJ, Sheedy PF II, Johnson CM, et al. Focal nodular hyperplasia and hepatic adenoma: comparison of angiography, CT, US, and scintigraphy. Radiology 1985; 156:593–595.
5. Carlson SK, Johnson CD, Bender CE, Welch TJ. CT of focal nodular hyperplasia of the liver. AJR Am J Roentgenol 2000; 174:705–712.
6. Mathieu D, Rahmouni A, Anglade MC, et al. Focal nodular hyperplasia of the liver: assessment with contrast-enhanced TurboFLASH MR imaging. Radiology 1991; 180:25–30.

7. Vogl TJ, Stupavsky A, Pegios W, et al. Hepatocellular carcinoma: evaluation with dynamic and static gadobenate dimeglumine-enhanced MR imaging and histopathologic correlation. Radiology 1997; 205:721–728.
8. Mattison GR, Glazer GM, Quint LE, Francis IR, Bree RL, Ensminger WD. MR imaging of hepatic focal nodular hyperplasia: characterization and distinction from primary malignant hepatic tumors. AJR Am J Roentgenol 1987; 148:711–715.
9. Caseiro-Alves F, Zins M, Mahfouz AE, et al. Calcification in focal nodular hyperplasia: a new problem for differentiation from fibrolamellar hepatocellular carcinoma. Radiology 1996; 198:889–892.
10. Choi CS, Freeny PC. Triphasic helical CT of hepatic focal nodular hyperplasia: incidence of atypical findings. AJR Am J Roentgenol 1998; 170:391–395.
11. Weimann A, Ringe B, Klempnauer J, et al. Benign liver tumors: differential diagnosis and indications for surgery. World J Surg 1997; 21:983–990.
12. Caudana R, Morana G, Pirovano GP, et al. Focal malignant hepatic lesions: MR imaging enhanced with gadolinium benzyloxypropionictetra-acetate (BOPTA)—preliminary results of phase II clinical application. Radiology 1996; 199:513–520.
13. Petersein J, Spinazzi A, Giovagnoni A, et al. Focal liver lesions: evaluation of the efficacy of gadobenate dimeglumine in MR imaging—a multicenter phase III clinical study. Radiology 2000; 215:727–736.
14. Seneterre E, Taourel P, Bouvier Y, et al. Detection of hepatic metastases: ferumoxides-enhanced MR imaging versus unenhanced MR imaging and CT during arterial portography. Radiology 1996; 200:785–792.
15. Mathieu D, Coffin C, Kobeiter H, et al. Unexpected MR-T1 enhancement of endocrine liver metastases with mangafodipir. J Magn Reson Imaging 1999; 10: 193–195.
16. Spinazzi A, Lorusso V, Pirovano G, Kirchin M. Safety, tolerance, biodistribution, and MR imaging enhancement of the liver with gadobenate dimeglumine: results of clinical pharmacologic and pilot imaging studies in nonpatient and patient volunteers. Acad Radiol 1999; 6: 282–291.
17. Kirchin MA, Pirovano GP, Spinazzi A. Gadobenate dimeglumine (Gd-BOPTA): an overview. Invest Radiol 1998; 33:798–809.
18. Grazioli L, Kirchin M, Pirovano G, Spinazzi A. MultiHance in the dynamic phase of contrast enhancement: a pictorial assessment. J Comput Assist Tomogr 1999; 23(suppl 1):S61–S64.
19. Pirovano G, Vanzulli A, Marti-Bonmati L, et al. Evaluation of the accuracy of gadobenate dimeglumine-enhanced MR imaging in the detection and characterization of focal liver lesions. AJR Am J Roentgenol 2000; 175:1111–1120.
20. Nguyen BN, Flejou JF, Terris B, Belghiti J, Degott C. Focal nodular hyperplasia of the liver: a comprehensive pathologic study of 305 lesions and recognition of new histologic forms. Am J Surg Pathol 1999; 23:1441–1454.
21. Rofsky NM, Weinreb JC, Bernardino ME, Young SW, Lee JK, Noz ME. Hepatocellular tumors: characterization with Mn-DPDP-enhanced MR imaging. Radiology 1993; 188:53–59.
22. Paley MR, Mergo PJ, Torres GM, Ros PR. characterization of focal hepatic lesions with ferumoxides-enhanced T2-weighted MR imaging. AJR Am J Roentgenol 2000; 175:159–163.
23. Cavagna FM, Maggioni F, Castelli PM, et al. Gadolinium chelates with weak binding to serum proteins: a new class of high-efficiency, general purpose contrast agents for magnetic resonance imaging. Invest Radiol 1997; 32:780–796.
24. Knopp MV, von Tengg-Kobligk H, Floemer F, Schoenberg SO. Contrast agents for MRA: future directions. J Magn Reson Imaging 1999; 10:314–146.
25. Hamm B, Kirchin M, Pirovano G, Spinazzi A. Clinical utility and safety of MultiHance in magnetic resonance imaging of liver cancer: results of multicenter studies in Europe and the USA. J Comput Assist Tomogr 1999; 23(suppl 1):S53–S60.
26. Grazioli L, Morana G, Caudana R, et al. Hepatocellular carcinoma: correlation between gadobenate dimeglumine-enhanced MRI and pathologic findings. Invest Radiol 2000; 35:25–34.
27. Leese T, Farges O, Bismuth H. Liver cell adenomas. Ann Surg 1998; 208:558–564.
28. Murakami T, Baron RL, Peterson MS, et al. Hepatocellular carcinoma: MR imaging with mangafodipir trisodium (Mn-DPDP). Radiology 1996; 200:69–77.
29. Denys A, Arrive L, Servois V, et al. Hepatic tumors: detection and characterization at 1-T MR imaging enhanced with AMI-25. Radiology 1994; 193:665–669.